Engineered Science
DOI: https://dx.doi.org/10.30919/es8d809

Iron-based Soft Magnetic Materials Fabricated by Laser Additive Manufacturing

Hengtong Wang,[1] Wen Feng,[4] Dong Liu,[2] Guodong Zhang,[1] Yao Liu,[1,*] Jun Wang[2] and Liang Zou[3,*]

Abstract

In the present study, soft magnetic materials were prepared by coating an Fe-based magnetic powder core with inorganic insulating materials such as phosphoric acid, manganese nitrate, and sodium molybdate. The prepared iron-based powders were effectively printed and shaped by laser additive manufacturing. The composition and microstructure of the soft magnetic materials were analyzed to assess changes in the magnetic properties. Compared with those of the samples prepared by traditional molding, these samples prepared by laser additive manufacturing exhibit excellent magnetic properties, including good saturation magnetic induction (1.6 T), magnetic permeability (μ_m=1923), and saturation magnetization (203.69 emu/g). The comprehensive properties of soft magnetic composites are improved by changing the composition of the phosphoric acid passivation solution. It is found that the coercivity of iron-based soft magnetic materials formulated by phosphoric acid passivation solution containing manganese nitrate and sodium molybdate was obviously reduced to 154.6 A/m.

Keywords: Iron powder; Soft magnetic materials; Magnetic properties; Laser additive manufacturing
Received: 10 September 2022; Revised: 03 December 2022; Accepted: 23 January 2023.
Article type: Research article.

1. Introduction

It is well established that soft magnetic materials hold great potential for miniaturization and intelligentization of electronic information industry. Nowadays, excellent properties of soft magnetic materials are actually highly desired to promote their practical development in multifunctional applications.[1-3] The soft magnetic materials prepared by rational design feature the characteristics of excellent magnetic properties and good processing properties. In addition, introducing insulation coating can evidently improve the resistivity of the material and remarkably reduce eddy current loss with energy saving, playing an indispensable role in economic development and even in military and civilian science and technology fields.[4-6] It is worth noting that iron powder is a soft magnetic material with a low price and is easy to obtain,[7] which is an ideal candidate as the magnetic core of the matrix in this paper. Benefiting from favorable magnetic properties and machinability, it is invested in electrical, power, and electronic equipment, such as electromagnet core, circuit breaker core, transformer core, motor stator, rotor core, and so on.[8-10] However, the further improvement of soft magnetic materials is still restricted by eddy current loss, which is mainly due to the increase in the applicable frequency of soft magnetic materials, resulting in an increase in eddy current losses.[11-14] To this end, it is necessary to choose suitable insulating coating material and forming process to produce soft magnetic composites with lower magnetic loss and superior magnetic properties. Recently, additive manufacturing, also known as 3D printing technology, has achieved substantial and significant advances. Applying the concept of calculus to discretize 3D solid model data into 2D cross-section data, it scans and accumulates the 2D cross-section data in the direction of height, finally

[1] *Key Laboratory for Liquid-Solid Structural Evolution and Processing of Materials (Ministry of Education), Shandong University, Jinan, 250061, China*
[2] *Shandong Tianhou New Material Technology Co. Ltd. Heze, Shandong, 274051, China*
[3] *Electrical Engineering Department, Shandong University, Jinan 250061, China*
[4] *Innovation Development Research Institute of Shandong Province.*
[*] *Email:* liuyao@sdu.edu.cn (Y. Liu); zouliang@sdu.edu.cn (L. Zou)

forming 3D solid parts.[15-19] The application of 3D printing technology not only brings great changes to practical production and our modern life but also shows favorable potential in many fields with a positive effect in the manufacturing of metal parts.[20-22] Recently, Garibaldi *et al*.[23] have investigated the SLM-processed high silicon steel and indicated that this process could be one of the promising methods to manufacture the soft magnetic component with complex morphology. Additionally, Zhang *et al*.[24] did the parametrical analysis with the SLM-processed Fe-Ni alloys for obtaining high relative density components.

Since the advantages of phosphating technology in practical production, such as strong operability, simple and mature formula, and low cost, phosphating solution passivation was selected to coast the iron matrix and obtain soft magnetic materials. The addition of manganese nitrate can increase the resistivity of the passivated iron powder and the thermal stability of the insulating coating was greatly improved. When sodium molybdate was added, a molybdate coating with magnetic properties was formed, which can effectively reduce the magnetic dilution of soft magnetic materials. By changing the composition of the phosphoric acid passivation solution, the comprehensive properties of soft magnetic materials could be greatly improved. In this work, the phosphoric acid-coated Fe-based soft magnetic materials were successfully prepared by laser additive manufacturing. The magnetic properties of 3D printed samples were compared with those of traditional molding, and the possibility of using 3D laser to print soft magnetic materials was also explored. Compared with Kocsis *et al*.,[25] the composition of phosphorylate was optimized and the magnetic performance was tested. However, the effect of different laser power on the microstructure was not investigated. We are planning to prepare ring samples with different laser power in future research to study the influence of laser power parameters on soft magnetic properties.

2. Experimental

2.1 Materials

The matrix material of the soft magnetic materials was reduced iron powder with an average particle size of about 100 μm, which was purchased from Shanghai Aladdin Biochemical Technology Co. Ltd. Zinc stearate. Manganese nitrate (50 wt%) and sodium molybdate were ordered from McLean Reagents, and phosphoric acid (85 wt%) was purchased from Sinopharm Chemical Reagents Co. Ltd.

2.2 Fabrication

The reduced iron powder was washed with deionized water and anhydrous ethanol. Four different phosphating solutions were prepared to passivate iron powder, and manganese ions and molybdate ions were introduced to synthesize soft magnetic composites. The components of four phosphating solutions are listed as follows: 1. Phosphoric acid solution with only phosphoric acid (1g) was added into the solute; 2. Manganese nitrate solution (2.3 g) was added into the phosphoric acid solution, and manganese ions were introduced; 3. Sodium molybdate (2 g) was added into the phosphoric acid solution, and molybdate ions were introduced; 4. Sodium molybdate (2 g) was first added to the phosphoric acid solution, and after a period of reaction, a manganese nitrate solution (2.3 g) was added. Two ions, manganese ion and molybdate radical, were introduced at the same time. Therefore, the raw material addition ratio of phosphoric acid and sodium molybdate is 1:2, and the raw material ratio of phosphoric acid and manganese nitrate is 1:2.3. The surface produces an approximate reactant ion ratio.

In order to enable the passivation of iron powder, the cleaned iron powder was added to the phosphating solution at 50 ℃, and the mechanical stirring was carried out for 30 min to achieve a uniform chemical reaction. Afterward, the phosphating solution remaining on the iron powder surface was washed with deionized water, and the passivated iron powder was gained after drying under a vacuum condition at 50 ℃.

After drying, the powder sample was divided into two parts, one of which was mixed with 0.2% zinc stearate as the release agent and put into an annular mold (36×40×10 mm). The prepared powder material was pressed into the annular mold, which was obtained by fixed pressure (800 MPa for 9 s), and then the samples were annealed in a tube furnace to allow reaction in an N_2 atmosphere at 550 ℃ for 30 min. Fig. 1 shows the schematic preparation illustration of 3D printed samples using a laser printer (4000 W fiber laser, IPG, Germany), into which another part of the prepared iron powder was put. The high-performance laser scanning machine was layered according to the 3D computer-aided design model so that the height of each laser scanning layer is 60 μm. The laser cladding was carried out clockwise at a speed of 0.01 m/s and then anticlockwise, alternately. After the printing was completed, the sample was cut off from the manganese steel plate platform, and the unnecessary slag skin was removed to obtain a 36×40×10 mm annular sample. Table 1 summarized the process parameter values programmed in this study. For simplicity, PO_4^{3-}, Mn^{2+}, MoO_4^{2-} and Mn^{2+}+MoO_4^{2-} represent H_3PO_4, H_3PO_4+$Mn(NO_3)_2$, H_3PO_4+Na_2MoO_4 and H_3PO_4+$Mn(NO_3)_2$+Na_2MoO_4, respectively.

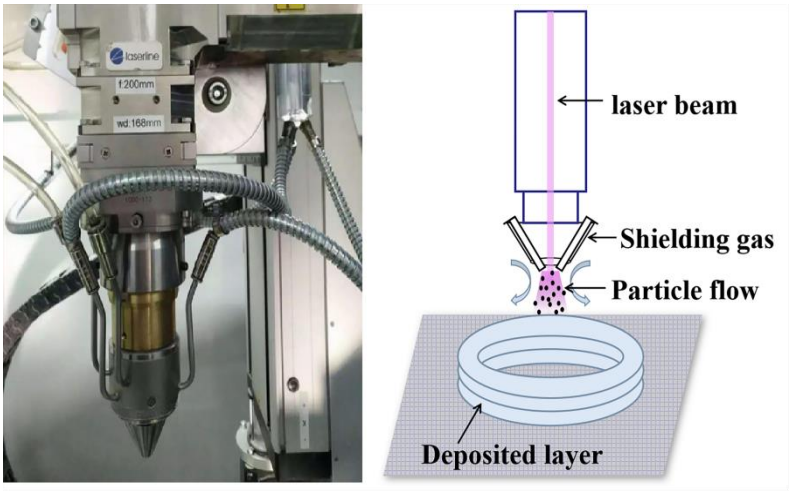

Fig. 1 Schematic diagram of laser 3D printing device.

Table 1. Selected build parameters for processing of annular specimens.

Build Parameters		
Power	P [W]	1100
Scan speed	v [mm/s]	10
Focal position	Δz [mm]	13.1
Layer thickness	d_h [μm]	60

2.3 Characterization methods

The phase composition of the soft magnetic materials was analyzed by an X-ray diffraction analyzer (XRD, DMAX-2500PC). The soft magnetic materials were observed by scanning electron microscope (SEM, JSM-7800F). The composition of the passivated film was studied by Fourier transform infrared spectrometer (FTIR, Nicolet 5700). The hysteresis loops of the samples were measured using a vibrating sample magnetometer (VSM, Quantum Design). The magnetic properties of annular samples, including coercivity (H_C), initial permeability (μ_i), saturation magnetic induction (B_S), and maximum permeability (μ_m) were measured by automatic measuring equipment for magnetic materials (MATS-2010SD/A), and the applied magnetic field and the frequency are 1 T and 200 Hz, respectively.

3. Results and discussion

3.1 Microstructure analysis

The samples of iron powder passivated by four different phosphating solutions were analyzed by XRD, and their characteristic diffraction patterns were depicted in Fig. 2(a). The signal peaks of iron were found at diffraction angles (2θ) of approximately 44.68, 65.06, and 82.34° (JCPDS 89-7194), and other diffraction peaks were not found, which is mainly due to the fact that the amount of molybdate coating and Fe-P and Mn-P phosphate generated on the iron powder surfaces is too limited to be detected.[26] The changes in the surface composition of iron powder treated with phosphoric acid were further studied by FTIR spectra. As shown in Fig. 2(b), the passivated film of phosphoric acid displays three characteristic bands, including phosphate hydrogen radical (HPO_4^{2-}) at 1642 cm^{-1}, phosphate radical (PO_4^{3-}) at 1046 cm^{-1} and 1380 cm^{-1}, and the peak at 3337 cm^{-1} are designated as O-H vibration signals.

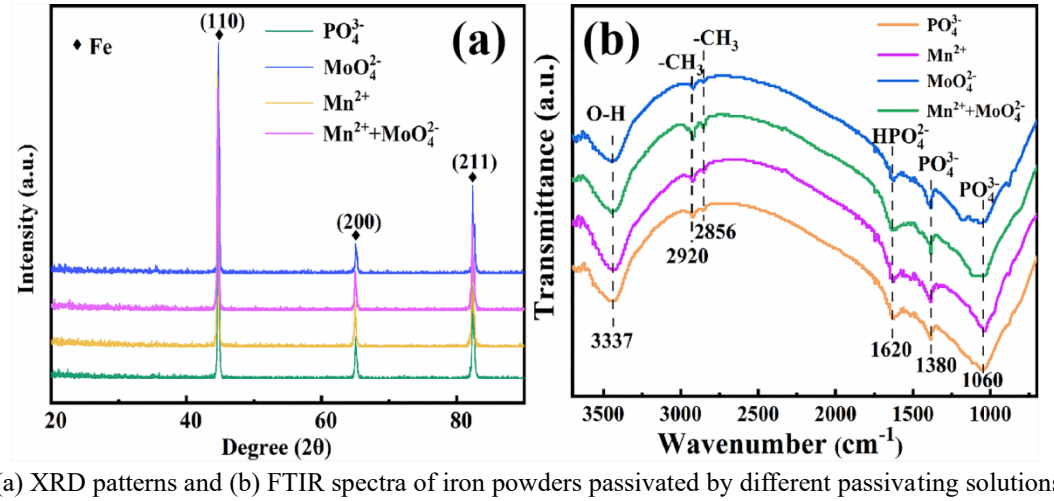

Fig. 2 (a) XRD patterns and (b) FTIR spectra of iron powders passivated by different passivating solutions.

The microstructure of powder samples in passivation solution with various components was investigated by SEM observation, as shown in Fig. 3. Compared with the pure iron powder in Fig. 3(a), Figs. 3(b)-(e) obviously shows that after passivation by phosphating solution, the surfaces of iron powder became rough, and flocculent structure appeared, indicating that a passivation film had been generated on the iron powder surfaces after passivation by phosphating solution. Compared with the passivation solution where only phosphoric acid was added as a solute, the passivation layers generated on the iron powder surfaces using that with manganese nitrate and sodium molybdate changed and formed a tight network structure, indicating that the passivation effect was well optimized. Combined with the coating layer generated on the iron powder surfaces evidenced by Fig. 3 and equations (1) and (4), it is proved that, in addition to Fe-P and Mn-P phosphate coating, molybdate insulation coating was also realized on the iron powder surfaces in the sample. Notably, NO_3^- is highly oxidizing in an acidic environment. It can be known clearly from equation (2) that NO_3^- can oxidize Fe^{2+} to Fe^{3+}. According to equations (3) and (4), magnetic $Fe_2(MoO_4)_3$ and $MnMoO_4$ could be formed as prominent components in molybdate coating. As for the reaction process, sodium molybdate and manganese nitrate were introduced into the phosphoric acid passivation solution. Except for the deposits generated by phosphate ions with iron and manganese ions, it was proposed that the remaining ions reacted as follows.[27,28]

$$Fe^{2+}+MoO_4^{2-}=FeMoO_4\downarrow \quad (1)$$

$$3Fe^{2+}+4H^{+}+NO_3^{-}=3Fe^{3+}+NO\uparrow+2H_2O \quad (2)$$

$$2Fe^{3+}+3MoO_4^{2-}=Fe_2(MoO_4)_3\downarrow \quad (3)$$

$$Mn^{2+}+MoO_4^{2-}=MnMoO_4\downarrow \quad (4)$$

When manganese ion was introduced into the phosphoric acid passivating solution, the resistivity of passivating iron powder increased, and the thermal stability of the insulating coating can be exceedingly improved. When molybdate ions were introduced, the molybdate coating with magnetic properties formed, which can effectively reduce the magnetic dilution of the soft magnetic materials. When manganese ions and molybdate ions were introduced into the passivation solution at the same time, the Fe-based soft magnetic materials could bond the merits of the two ions, delivering excellent magnetic properties.

The internal microstructure of the soft magnetic materials is quite significant for their properties, especially the magnetic properties. The microstructure of the soft magnetic materials produced by laser additive manufacturing is not only affected by its material composition but also strongly related to the parameters during the additive manufacturing fabrication process. The internal manufacturing defects (including pores and cracks), microstructure characteristics, and residual stress present a complex influence on the magnetic properties of the laser additive manufacturing parts. When a magnetic field is applied to the magnetic alloy, the internal spin and orbital motions of electrons would respond to the magnetic field, which is called magnetization. The domains move or change along the direction of the external magnetic field, and they also respond when the magnetic field is removed, which is called demagnetization. In these two processes, the domain walls would move with the motion of the domain. The manufacturing defects lead to local pinning sites during magnetization or demagnetization, hindering the movement of

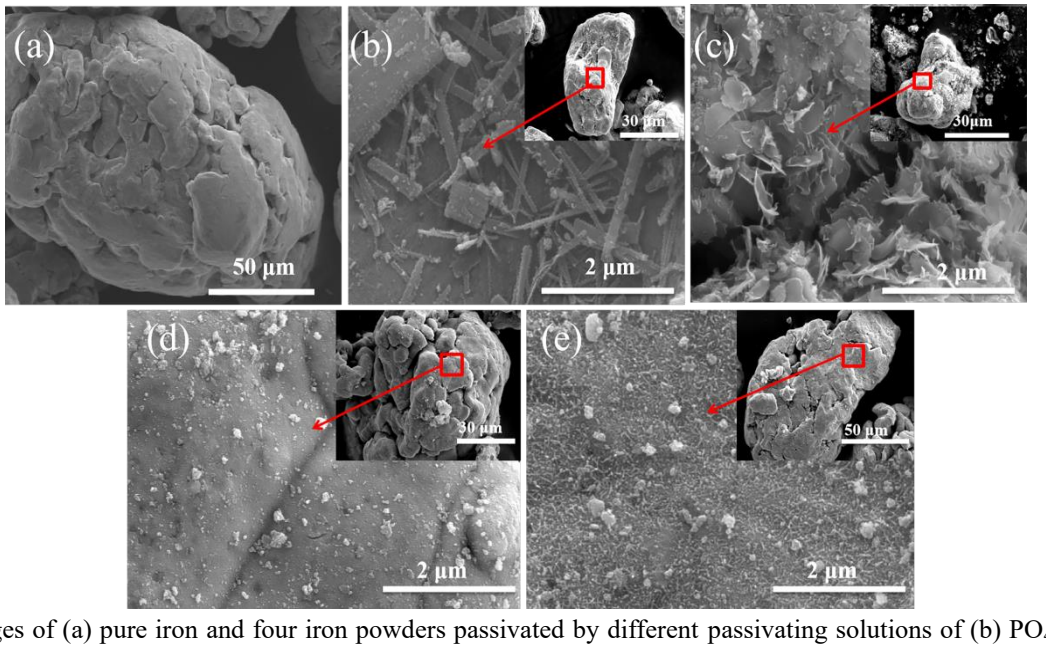

Fig. 3 SEM images of (a) pure iron and four iron powders passivated by different passivating solutions of (b) PO_4^{3-}, (c) Mn^{2+}, (d) MoO_4^{2-} and (e) Mn^{2+}+MoO_4^{2-}.

domain walls. The related magnetic properties such as coercivity, remanence, and power losses are damaged due to the pining sites of the domain wall motion.[29] The cross-section interface micrographs in Fig. 4 show the grain structure in the horizontal plane of the samples after annealing at 550 ℃.

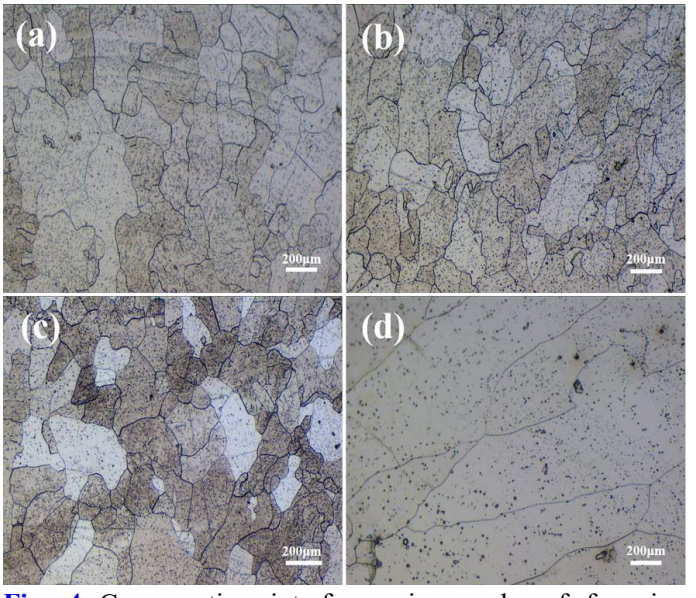

Fig. 4 Cross-section interface micrographs of four iron powders passivated by different passivating solutions with (a) PO_4^{3-}, (b) Mn^{2+}, (c) MoO_4^{2-}, and (d) Mn^{2+}+MoO_4^{2-}.

As can be seen in Fig. 4, the Fe powder melted partially or completely, leading to a more compact structure. The increased energy intake, after a certain level, damaged the phosphate coating to such an extent that the electrically conductive portions were connected and formed a complete lattice structure. In Figs. 4(a) and (b), the microstructure appears partially recrystallized morphology. The recrystallization is thought to be driven by the relief of the laser-induced residual stresses, as suggested in the literature for other SLM-processed alloys, including iron and Inconel 718.[30] The main contributors to this process are grain boundaries and consequent grain size, nonmetallic inclusions, and internal stresses. The sample was characterized by a homogenized microstructure, characterized by non-uniform grain size. In particular, while the largest grains are predominantly equiaxed and present sizes up to 300 μm, much smaller grains with sizes below 50 μm are also visible, suggesting that the recrystallization process was not complete. In Fig. 4(d), the grain size is larger than those in Figs. 4(a), (b) and (c). The grain size and shape significantly differ from those found in Fe-based alloys with phase transformations in the solid state, as their structure after laser melting is martensitic-like plate one. Therefore, although it is not fully clear why recrystallization did not alter the as-built texture, it is believed that the as-built grains with a preferential orientation are more likely to grow by consuming the randomly oriented ones, due to the typically smaller size of the latter. Furthermore, it is possible that the recrystallization partially proceeded via the growth of nuclei that are preferentially oriented nucleation theory of recrystallization.

3.2 Magnetic properties characterization

The hysteresis loops of iron powder treated with phosphating solution are shown in Fig. 5. Compared with the sample containing phosphoric acid passivation, the sample containing manganese nitrate passivation solution exhibits the lowest saturation magnetization. The saturation magnetization (M_S) of the passivation solution with manganese nitrate and sodium molybdate reached the maximum value (203.69 emu/g). The magnetic dilution effects of nonmagnetic materials are different with the passivation solution composition added, and the enhanced magnetic dilution effect could apparently reduce the saturation magnetization intensity of the samples.[31] The values of density, remanence, and hardness of laser-processed samples were summarized in Table 2. When sodium molybdate and manganese nitrate were added to the phosphoric acid passivation solution, the density of the sample was the best, and the hardness reached the maximum value (116.17 HB) with the lowest remanence.

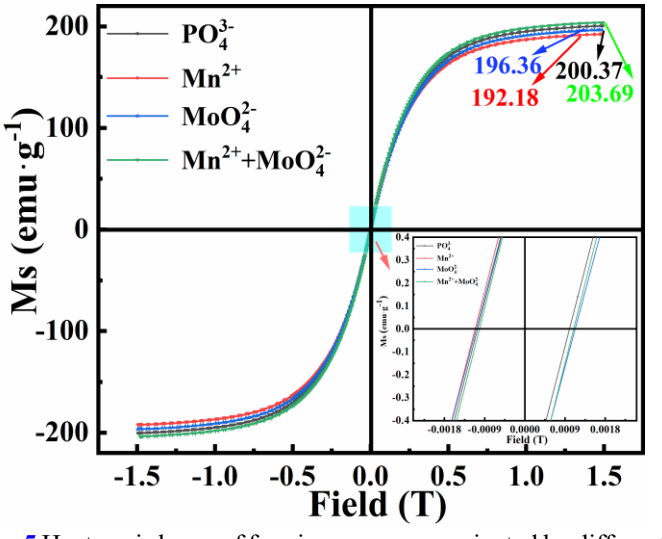

Fig. 5 Hysteresis loops of four iron powers passivated by different passivating solutions.

Table 2. The density, remanence and hardness of samples.

Samples	Density (g/cm^3)	Remanence (T)	Hardness (HB)
H_3PO_4	7.39	0.25	91.33
H_3PO_4+$Mn(NO_3)_2$	7.19	0.36	89.01
H_3PO_4+Na_2MoO_4	7.47	0.22	82.85
H_3PO_4+$Mn(NO_3)_2$+ Na_2MoO_4	7.48	0.17	116.17

In order to obtain excellent magnetic properties and mechanical properties, a proper heat treatment process is

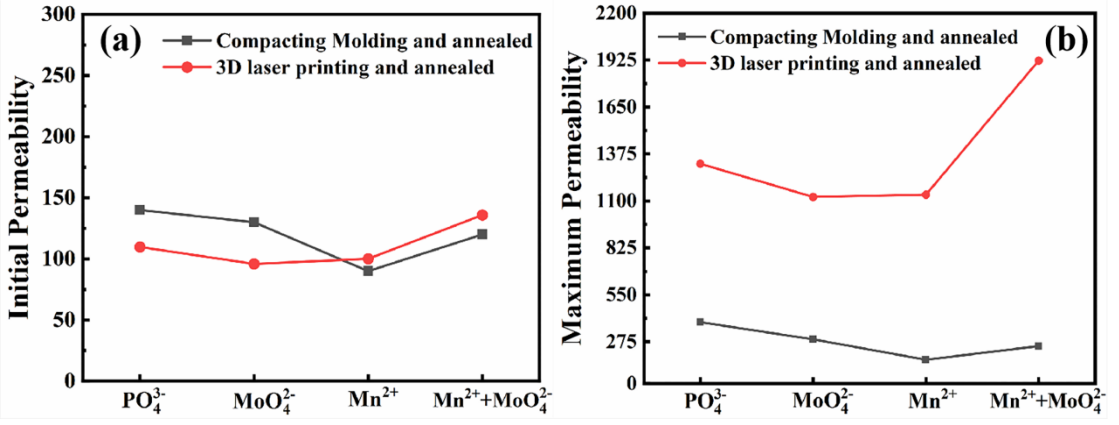

Fig. 6 Permeability of four iron powers passivated by different passivating solutions with (a) initial permeability and (b) the maximum permeability.

usually required for forming soft magnetic materials. Therefore, the laser-printed annular samples were annealed at 550 °C together with the traditional molded samples, and their magnetic properties were tested respectively. The initial permeability and the maximum permeability determine the energy conversion efficiency of the device. The saturation magnetic induction intensity determines whether the sample can meet the performance requirements of miniaturized products. The coercivity indicates how easily a material can be magnetized.[32-34] In addition to the inherent magnetic parameters of the material affecting the magnetism in the static magnetic field, the internal stress, porosity, and uniformity of the annular sample also largely affect the magnetic properties.[35]

As shown in Fig. 6(a), compared with the traditional molded samples in four different phosphoric acid passivation solutions, the initial permeability (μ_i) did not change much, while in Fig. 6(b) the maximum magnetic permeability (μ_m) increased significantly. When sodium molybdate and manganese nitrate were added to the phosphoric acid passivation solution, compared with the sample prepared by traditional molding, the maximum permeability of the sample increased from 251 to 1923, enhanced by 7.69 times. In addition, as shown in Fig. 7, compared with other soft magnetic materials prepared by 3D printing, the maximum permeability obtained in this work still displays obvious advantages.

Figure 8(a) shows the saturation magnetic induction of four iron powers passivated by different passivating solutions. It is founded that the saturation magnetic induction of the 3D-printed sample annealed at 550 °C is generally better. Compared with the samples prepared by traditional molding, the saturation magnetic induction increased from 1.2 to 1.6 T. The variation of coercivity is shown in Fig. 8(b), and the coercivity of the samples prepared by traditional molding is

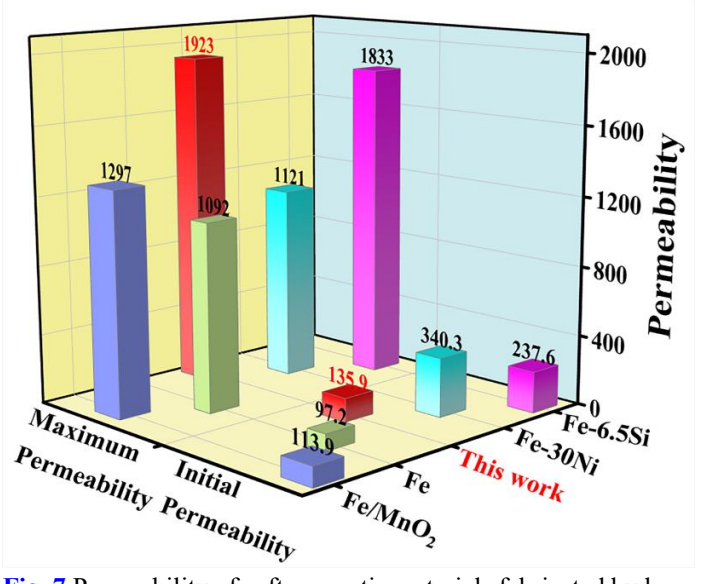

Fig. 7 Permeability of soft magnetic materials fabricated by laser additive manufacturing.

generally high, which is about 330 A/m. Among the phosphoric acid passivation solution samples containing manganese nitrate and sodium molybdate, the coercivity of the samples prepared by 3D printing was significantly reduced from 331.7 to 154.6 A/m. This is owing to the fact that coercivity largely depends on the particle size of the magnetic matrix, and the coercivity increases along with the decrease of the particle size. In this respect, it is supposed that the coercivity of laser-printed samples decreased obviously due to the dramatic grain growth.

4. Conclusion

The sample prepared by laser printing can be used effectively in a lower frequency range due to its compact structure, smaller coercivity, and superior magnetic permeability. Experience in the manufacturing process has shown that laser printing required a higher level of insulating cladding material

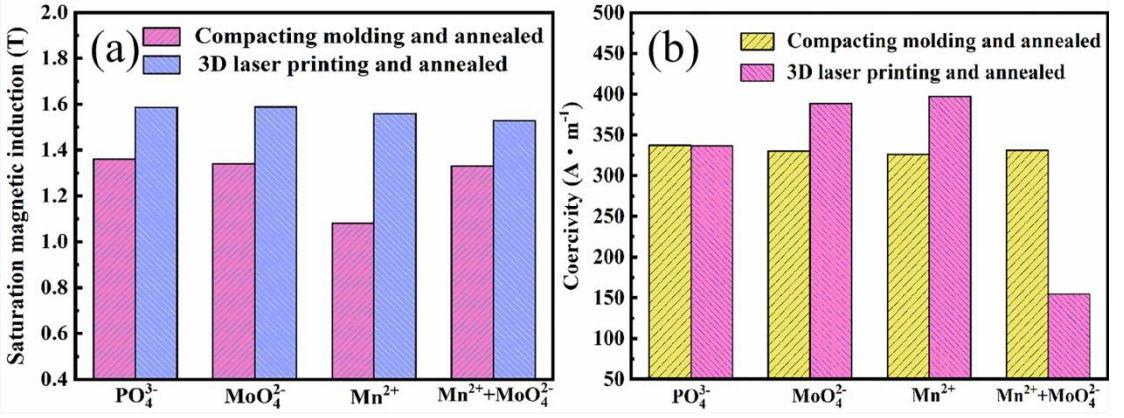

Fig. 8 (a) The saturation magnetic induction and (b) the coercivity of four iron powers passivated by different passivating solutions.

to ensure a compact structure with pleasant magnetic properties. Compared with the sample prepared by traditional molding, the magnetic permeability of the sample synthesized by 3D printing was significantly improved, and the coercivity was also reduced to a certain extent, which largely enhanced the overall magnetic property. The best magnetic properties were obtained by treating the samples with sodium molybdate and manganese nitrate, with a large permeability (μ_m=1923) and saturation magnetization (203.69 emu/g). It can be supposed that under the condition of high-temperature resistance of insulating cladding materials, soft magnetic materials can be prepared by using different cladding methods, and the annular sample can be printed by laser to reduce the magnetic loss.

Acknowledgments

The work was financially supported by the National Natural Science Foundation of China [grant No. 51771104, 51977122 and 51971119], the Shandong Natural Science Foundation for Excellent Young Scholars [grant No. ZR2020YQ32] and Project of Introducing Urgently Needed Talents in Key Supporting Regions of Shandong Province [grant No. 2203-371703-04-01-786537].

Conflict of Interest

There is no conflict of interest.

Supporting Information

Not applicable.

References

[1] S. Wu, A. Sun, F. Zhai, J. Wang, Q. Zhang, W. Xu, P. Logan, A. A. Volinsky, Annealing effects on magnetic properties of silicone-coated iron-based soft magnetic composites, *Journal of Magnetism and Magnetic Materials*, 2012, **324**, 818-822, doi: 10.1016/j.jmmm.2011.09.026.

[2] J. Wang, X.-A. Fan, Z. Wu, G. Li, Regulation and control of insulated layers for intergranular insulated Fe/SiO_2 soft magnetic composites, *Journal of Materials Science*, 2017, **52**, 7091-7099, doi: 10.1007/s10853-017-0941-9.

[3] E. A. Périgo, B. Weidenfeller, P. Kollár, J. Füzer, Past, present, and future of soft magnetic composites, *Applied Physics Reviews*, 2018, **5**, 031301, doi: 10.1063/1.5027045.

[4] S. X. Wang, N. X. Sun, M. Yamaguchi, S. Yabukami, Properties of a new soft magnetic material, *Nature*, 2000, **407**, 150-151, doi: 10.1038/35025142.

[5] E. Bayramli, O. Golgelioglu, H. B. Ertan, Powder metal development for electrical motor applications, *Journal of Materials Processing Technology*, 2005, **161**, 83-88, doi: 10.1016/j.jmatprotec.2004.07.070.

[6] Y. L. Zhang, X. A. Fan, W. T. Hu, Z. G. Luo, Z. J. Yang, G. Q. Li, Y. W. Li, Microstructure and magnetic properties of MnO_2 coated iron soft magnetic composites prepared by ball milling, *Journal of Magnetism and Magnetic Materials*, 2020, **514**, 167295, doi: 10.1016/j.jmmm.2020.167295.

[7] I. P. Gilbert, V. Moorthy, S. J. Bull, J. T. Evans, A. G. Jack, Development of soft magnetic composites for low-loss applications, *Journal of Magnetism and Magnetic Materials*, 2002, **242-245**, 232-234, doi: 10.1016/s0304-8853(01)01252-5.

[8] J. J. Zhong, Y. G. Guo, J. G. Zhu, Z. W. Lin, Characteristics of soft magnetic composite material under rotating magnetic fluxes, *Journal of Magnetism and Magnetic Materials*, 2006, **299**, 29-34, doi: 10.1016/j.jmmm.2005.03.016.

[9] F. Alves, R. Lebourgeois, T. Waeckerlé, Soft magnetic materials for electrical engineering: state of the art and recent advances, *European Transactions on Electrical Power*, 2005, **15**, 467-479, doi: 10.1002/etep.70.

[10] D. Liu, C. Wu, M. Yan, J. Wang, Correlating the microstructure, growth mechanism and magnetic properties of FeSiAl soft magnetic composites fabricated via HNO_3 oxidation, *Acta Materialia*, 2018, **146**, 294-303, doi: 10.1016/j.actamat.2018.01.001.

[11] H. Shokrollahi, K. Janghorban, Effect of warm compaction on the magnetic and electrical properties of Fe-based soft magnetic composites, *Journal of Magnetism and Magnetic Materials*, 2007, **313**, 182-186, doi: 10.1016/j.jmmm.2006.12.022.

[12] M. Anhalt, Systematic investigation of particle size dependence of magnetic properties in soft magnetic composites, *Journal of Magnetism and Magnetic Materials*, 2008, **320**, 10366-10369, doi: 10.1016/j.jmmm.2008.02.072.
[13] Z. Wei, Z. Wang, C. Xu, G. Fan, X. Song, Y. Liu, R. Fan, Defect-induced insulator-metal transition and negative permittivity in La1-Ba CoO_3 perovskite structure, *Journal of Materials Science & Technology*, 2022, **112**, 77-84, doi: 10.1016/j.jmst.2021.11.002.
[14] B. Y. Meng, J. X. Hou, F. Z. Ning, B. Yang, B. H. Zhou, R. H. Yu, Low-loss and high-induction Fe-based soft magnetic composites coated with magnetic insulating layers, *Journal of Magnetism and Magnetic Materials*, 2019, **492**, 165651, doi: 10.1016/j.jmmm.2019.165651.
[15] B. Bhushan, M. Caspers, An overview of additive manufacturing (3D printing) for microfabrication, *Microsystem Technologies*, 2017, **23**, 1117-1124, doi: 10.1007/s00542-017-3342-8.
[16] J. Gardan, Additive manufacturing technologies: state of the art and trends, *International Journal of Production Research*, 2015, **54**, 3118-3132, doi: 10.1080/00207543.2015.1115909.
[17] V. Chaudhary, S. A. Mantri, R. V. Ramanujan, R. Banerjee, Additive manufacturing of magnetic materials, *Progress in Materials Science*, 2020, **114**, 100688, doi: 10.1016/j.pmatsci.2020.100688.
[18] D. Bourell, J. P. Kruth, M. Leu, G. Levy, D. Rosen, A. M. Beese, A. Clare, *Materials for additive manufacturing*, CIRP Annals, 2017, **66**, 659-681, doi: 10.1016/j.cirp.2017.05.009.
[19] T. DebRoy, H. L. Wei, J. S. Zuback, T. Mukherjee, J. W. Elmer, J. O. Milewski, A. M. Beese, A. Wilson-Heid, A. De, W. Zhang, Additive manufacturing of metallic components - Process, structure and properties, *Progress in Materials Science*, 2018, **92**, 112-224, doi: 10.1016/j.pmatsci.2017.10.001.
[20] C. V. Mikler, V. Chaudhary, T. Borkar, V. Soni, D. Jaeger, X. Chen, R. Contieri, R. V. Ramanujan, R. Banerjee, Correction to: laser additive manufacturing of magnetic materials, *The Journal of The Minerals, Metals & Materials Society (TMS),* 2017, **69**, 2855-2856, doi: 10.1007/S11837-017-2623-0.
[21] M. Garibaldi, I. Ashcroft, J. N. Lemke, M. Simonelli, R. Hague, Effect of annealing on the microstructure and magnetic properties of soft magnetic Fe-Si produced via laser additive manufacturing, *Scripta Materialia*, 2018, **142**, 121-125, doi: 10.1016/j.scriptamat.2017.08.042.
[22] E. A. Périgo, J. Jacimovic, F. García Ferré, L. M. Scherf, Additive manufacturing of magnetic materials, *Additive Manufacturing*, 2019, **30**, 100870, doi: 10.1016/j.addma.2019.100870.
[23] J. N. Lemke, M. Simonelli, M. Garibaldi, I. Ashcroft, R. Hague, M. Vedani, R. Wildman, C. Tuck, Calorimetric study and microstructure analysis of the order-disorder phase transformation in silicon steel built by SLM, *Journal of Alloys and Compounds*, 2017, **722**, 293-301, doi: 10.1016/j.jallcom.2017.06.085.
[24] B. Zhang, N.-E. Fenineche, H. Liao, C. Coddet, Magnetic properties of in-situ synthesized $FeNi_3$ by selective laser melting Fe-80%Ni powders, *Journal of Magnetism and Magnetic Materials*, 2013, **336**, 49-54, doi: 10.1016/j.jmmm.2013.02.014.
[25] B. Kocsis, I. Fekete, I. Hatos, L. K. Varga, Soft magnetic composites prepared by 3D laser printing, *Acta Physica Polonica A*, 2020, **137**, 886-888, doi: 10.12693/aphyspola.137.886.
[26] G. Li, L. Niu, J. Lian, Z. Jiang, A black phosphate coating for C1008 steel, *Surface and Coatings Technology*, 2004, **176**, 215-221, doi: 10.1016/s0257-8972(03)00736-9.
[27] Y. Ding, Y. Wan, Y.-L. Min, W. Zhang, S.-H. Yu, General synthesis and phase control of metal molybdate hydrates $MMoO_4 \cdot nH_2O$ (M = Co, Ni, Mn, n = 0, 3/4, 1) nano/microcrystals by a hydrothermal approach: magnetic, photocatalytic, and electrochemical properties, *Inorganic Chemistry*, 2008, **47**, 7813-7823, doi: 10.1021/ic8007975.
[28] S. Rebeyrat, J. L. Grosseau-Poussard, P. O. Renault, B. Panicaud, J. F. Dinhut, Structural characterisation of phosphated α-iron oxidised at 400 °C, *Surface and Coatings Technology*, 2002, **161**, 144-149, doi: 10.1016/s0257-8972(02)00361-4.
[29] S. Gao, X. Yan, C. Chang, E. Aubry, M. Liu, H. Liao, N. Fenineche, Effect of laser energy density on surface morphology, microstructure, and magnetic properties of selective laser melted Fe-3wt.% Si alloys, *Journal of Materials Engineering and Performance*, 2021, **30**, 5020-5030, doi: 10.1007/s11665-021-05591-w.
[30] W. J. Sames, F. A. List, S. Pannala, R.R. Dehoff, S. S. Babu, The metallurgy and processing science of metal additive manufacturing, *International Materials Reviews*, 2016, **61**, 315-360, doi: 10.1080/09506608.2015.1116649.
[31] Y. Chen, L. Zhang, H. Sun, F. Chen, P. Zhang, X. Qu, E. Fan, Enhanced magnetic properties of iron-based soft magnetic composites with phosphate-polyimide insulating layer, *Journal of Alloys and Compounds*, 2020, **813**, 152205, doi: 10.1016/j.jallcom.2019.152205.
[32] A. H. Taghvaei, H. Shokrollahi, K. Janghorban, Properties of iron-based soft magnetic composite with iron phosphate–silane insulation coating, *Journal of Alloys and Compounds*, 2009, **481**, 681-686, doi: 10.1016/j.jallcom.2009.03.074.
[33] S. Wu, A. Z. Sun, Z. W. Lu, C. Cheng, X. X. Gao, Magnetic properties of iron-based soft magnetic composites with SiO_2 coating obtained by reverse microemulsion method, *Journal of Magnetism and Magnetic Materials*, 2015, **381**, 451-456, doi: 10.1016/j.jmmm.2015.01.030.
[34] R. Nowosielski, J. J. Wyslocki, I. Wnuk, P. Gramatyka, Nanocrystalline soft magnetic composite cores, *Journal of Materials Processing Technology*, 2006, **175**, 324-329, doi: 10.1016/j.jmatprotec.2005.04.017.
[35] G. D. Zhang, G. Y. Shi, W. T. Yuan, Y. Liu, Magnetic properties of iron-based soft magnetic composites prepared via phytic acid surface treatment, *Ceramics International*, 2021, **47**, 8795-8802, doi: 10.1016/j.ceramint.2020.11.245.

